International Journal of Computational Methods
Vol. 12, No. 3 (2015) 1550015 (15 pages)

DOI: 10.1142/S0219876215500152

World Scientific
www.worldscientific.com

A Scheme For Inviscid Compressible Flow, Considering A Gas In Thermo–Chemical Equilibrium

J. Saldia
Department of Aeronautics, National University of Córdoba
National Scientific and Technical Research Council (CONICET), Argentina
jsaldia@conicet.gov.ar

S. Elaskar
Department of Aeronautics, National University of Córdoba
National Scientific and Technical Research Council (CONICET), Argentina

J. Tamagno
Department of Aeronautics, National University of Córdoba

Received 7 June 2013
Revised 19 June 2014
Accepted 16 December 2014
Published 26 May 2015

A finite volume scheme for the solution of the unsteady 1D Euler equations, considering the working gas in thermo-chemical equilibrium, is presented. To achieve total variation diminishing (TVD) properties in the numerical scheme, a technique proposed by the co-authors, based on the use of different limiter functions in each wave of the Riemann problem, is applied. By proper selection of the limiter functions, the unwanted effects of the numerical viscosity on the capture of contact discontinuities are reduced, but without losing robustness in shock waves resolution. With the aim of evaluating the developed numerical scheme, results obtained solving several Riemann problems, specially selected for this specific purpose, are presented.

Keywords: Euler equations; TVD schemes; chemical equilibrium.

1. Introduction

In solving the Euler equations, physical discontinuities may arise. Its accurate and robust numerical resolution, represents a constant challenge in the development of new methods. It is well known that second-order schemes solve these discontinuities accurately, but present the shortcoming of generating oscillations in the solution around them. On the other hand, first-order schemes do not generate oscillations,

but tend to smear the discontinuities excessively. A class of high-order schemes known as total variation diminishing (TVD), have the mathematical property of not introducing new extrema in the solution, solving with high precision the discontinuities without generating oscillations. Nevertheless, the TVD condition has only been proven in the scalar convection equation [Harten *et al.* (1983b)]. Thus, if applied to systems of nonlinear equations, TVD schemes may not be oscillations free. When applying the TVD scheme originally devised by Harten [Harten *et al.* (1983b)] and later modified and generalized by Yee [Yee *et al.* (1985); Yee (1987a, 1987b, 1989)] to the numerical solution of the Euler equations system, it is well known that the discontinuities associated to the linearly degenerated wave family, e.g., contact discontinuities, are very hard of solving accurately, unless that highly compressive limiter functions are used. However, compressive limiter functions have a series of disadvantages: Lack of robustness in the capture of shock waves, [Hirsch (1992)], nonfree unphysical oscillations solutions and poor convergence rates and poor numerical stability in 2D and 3D steady state calculations [Zheng and Lee (1998)], in addition to others.

In a previous paper [Falcinelli *et al.* (2008)], we have proposed an adaptive inclusion of limiter functions in the context of the Harten–Yee TVD scheme. In this technique, if under an established comparison criteria, the strength of the linearly degenerate waves family are higher than the strength of the genuinely nonlinear waves family, then a highly compressive limiter function, know as *superbee*, is applied with the linearly degenerate wave family. Otherwise, the original upwind scheme of Yee, which uses the more diffusive *minmod* limiter function in all waves is employed. This adaptive modification has shown ability in solving quite accurately contact discontinuities without losing robustness in capturing shock waves. The aim of this work is to extend the just mentioned adaptive technique in solving the 1D Euler equations system, assuming that the working gas in thermo–chemical equilibrium.

Results obtained solving the 1D Riemann problem in several cases specially designed to enhance the differences between equilibrium states an its perfect caloric counterpart are presented. Through this cases, three alternatives of selection of limiter functions are compared and evaluated. The natural motivation for the applications of the numerical adaptive scheme here presented, is its future extension to the solution of 2D and 3D Euler equations in the hypersonic flight regime, where chemical equilibrium gas assumptions allows to make more accurate predictions of important design variables, as for example, the surface temperature distribution over bodies [Anderson (1989)].

2. System of Equations

2.1. *Euler equations*

The Euler equations form a nonlinear hyperbolic system of differential equations, that describe the dynamics of a compressible fluid flow disregarding the effects of mass forces, viscosity, and heat transfer by conduction and radiation. The 1D Euler

equations may be written in conservation form as:

$$\frac{\partial \mathbf{U}}{\partial t} + \frac{\partial \mathbf{F}(\mathbf{U})}{\partial x} = \mathbf{0}, \tag{1a}$$

$$\mathbf{U} = \begin{pmatrix} \rho \\ \rho u \\ E \end{pmatrix}, \quad \mathbf{F} = \begin{pmatrix} \rho u \\ \rho u^2 + p \\ u(E+p) \end{pmatrix}, \tag{1b}$$

where ρ is the density, u is the velocity, and E is the total energy of the flow defined by

$$E = \rho\left(\frac{1}{2}u^2 + e\right). \tag{2}$$

In this work, the closure of the Euler equations systems is provided by solving the chemical equilibrium state of the fluid, assuming that the fluid is a mixture of thermally perfect gases that obeys the equation of state,

$$p = \rho\frac{R}{W}T, \tag{3}$$

where R is the universal gas constant, T is the thermodynamic temperature and W is the molecular weight of the gas mixture given by the chemical equilibrium composition.

3. Numerical Discretization

3.1. *TVD scheme*

The integral form of the system (1) is discretized following the usual finite volume formulation [Hirsch (1992)]:

$$\frac{d\mathbf{U}_i}{dt} = -\frac{1}{\Delta x}(\mathbf{F}_{i+\frac{1}{2}} - \mathbf{F}_{i-\frac{1}{2}}). \tag{4}$$

The numerical flux function employed corresponds to the Harten's TVD scalar scheme originally devised by [Harten *et al.* (1983b)], and extended to system of equations by Yee [Yee *et al.* (1985); Yee (1987)]:

$$\mathbf{F}_{i+\frac{1}{2}} = \frac{1}{2}(\mathbf{F}_i + \mathbf{F}_{i+1}) + \frac{1}{2}\mathbf{R}_{i+\frac{1}{2}}\mathbf{\Phi}_{i+\frac{1}{2}}, \tag{5}$$

where the notation $\mathbf{F}_i \equiv \mathbf{F}(\mathbf{U}_i)$ was employed. The l-column of the matrix $\mathbf{R}_{i+\frac{1}{2}}$ corresponds to the right eigenvector associated to the l-eigenvalue $\lambda_{i+\frac{1}{2}}$ of the Jacobian matrix $\mathbf{A}(\mathbf{U}) = \frac{\partial \mathbf{F}}{\partial \mathbf{U}}$ evaluated at an average state $\mathbf{u}_{i+\frac{1}{2}}$. In this work, we employ the Roe's average state [Roe (1981)] for the linearization of the Jacobian matrix and the evaluation of its eigenvalues and eigenvectors. The complete definition of the Roe's average state for gases that do not obey a perfect equation of state is accomplished through the technique proposed by [Vinokur and Montagné (1990)], see also [Mottura *et al.* (1997)] for further details.

The components of $\mathbf{\Phi}_{i+\frac{1}{2}}$ in (5) are defined by:

$$\Phi^l_{i+\frac{1}{2}} = \sigma(\lambda^l_{i+\frac{1}{2}})(g^l_i + g^l_{i+1}) - \psi(\lambda^l_{i+\frac{1}{2}} + \gamma^l_{i+\frac{1}{2}})\alpha^l_{i+\frac{1}{2}}. \tag{6}$$

The $\alpha^l_{i+\frac{1}{2}}$ in (6) are the components of the spectral decomposition vector $\boldsymbol{\alpha}_{i+1}$ of the Riemann problem at cell interfaces and are given by,

$$\boldsymbol{\alpha}_{i+\frac{1}{2}} = \mathbf{R}^{-1}_{i+\frac{1}{2}}(\mathbf{U}_{i+1} - \mathbf{U}_i). \tag{7}$$

For accurate temporal calculations $\sigma(z)$ is defined in [Yee (1989)] by

$$\sigma(z) = \frac{1}{2}\left(\psi(z) - \frac{\Delta t}{\Delta x} z^2\right), \tag{8}$$

where $\psi(z)$ is necessary to guarantee the scheme convergence toward the physically relevant solution [Harten *et al.* (1983a)] and is defined by,

$$\psi(z) = \begin{cases} |z| & \text{if } |z| \geq \delta_1 \\ \dfrac{(z^2 + \delta_1^2)}{2\delta_1} & \text{if } |z| < \delta_1, \end{cases} \tag{9}$$

where δ_1 is a small and positive parameter, that may be dependent on the solution.

The scalar function g^l_i in (6) is known as the flux limiter function, closely related with the TVD property of the scheme. In the selection of the limiter functions, we employ the methodology proposed by [Falcinelli *et al.* (2008)]. In this technique, the superscript l in (6) is considered to be associated either to a linearly degenerated family or to a genuinely nonlinear family of characteristic waves of the hyperbolic system of equations. Then, the strength of the spectral decomposition vector components are compared under a certain imposed comparison criteria. If the strength of those components associated to the linearly degenerated family are higher than the corresponding to the genuinely nonlinear, the *superbee* [Roe (1986)] limiter function is employed with those $l's$ associated to the linearly degenerated family, and the *minmod* limiter function [Sweby (1984)] with the rest. Otherwise, the *minmod* limiter is used with all waves. This methodology aims to take advantage of what does each limiter function best, that is, getting robustness and absence of oscillations with the *minmod* function, and high resolutions in contact discontinuities with the *superbee* function.

In this work, the wave strengths at the interface $I^l_{i+\frac{1}{2}}$ are evaluated through the modulus of the difference of conservative variables between the states separated by the characteristic waves associated with the local Riemann problem:

$$I^l_{i+\frac{1}{2}} = \|\alpha^l_{i+\frac{1}{2}} \mathbf{R}^l_{i+\frac{1}{2}}\|. \tag{10}$$

The *minmod* limiter function is defined by

$$g^l_i = S \cdot \max[0, \min(|\alpha^l_{i+\frac{1}{2}}|, S \cdot \alpha^l_{i-\frac{1}{2}})], \quad S = \text{sign}(\alpha^l_{i+\frac{1}{2}}) \tag{11}$$

and, the *superbee* function by

$$g_i^l = S \cdot \max[0, \min(2|\alpha_{i+\frac{1}{2}}^l|, S \cdot \alpha_{i-\frac{1}{2}}^l), \ldots$$
$$\min(|\alpha_{i+\frac{1}{2}}^l|, 2S \cdot |\alpha_{i-\frac{1}{2}}^l|)], \quad S = \mathrm{sgn}(\alpha_{i+\frac{1}{2}}^l). \tag{12}$$

Finally, with the description of the function,

$$\gamma_{i+\frac{1}{2}}^l = \sigma(\lambda_{i+\frac{1}{2}}^l) \begin{cases} \dfrac{(g_{i+1}^l - g_i^l)}{\alpha_{i+\frac{1}{2}}^l} & \text{if } \alpha_{i+\frac{1}{2}}^l \neq 0 \\ 0 & \text{if } \alpha_{j+\frac{1}{2}}^l = 0 \end{cases} \tag{13}$$

all components of $\mathbf{\Phi}_{i+\frac{1}{2}}$ are defined.

4. Results

4.1. *Test cases*

A total of five 1D Riemann problems are presented. These test cases have been previously used by [Montagné *et al.* (1989); Yee (1989)] to compare the performances of TVD schemes where the gas is considered in chemical equilibrium. The initial conditions of the state at the left (L) and right (R) of the initial discontinuity for each of the test cases are given in Table 1. In all cases, the working gas is air with the following molar percentage composition: ($N_2 = 78.084, O_2 = 20.9476, Ar = 0.9365, CO_2 = 0.0319$). The chemical equilibrium gas properties are computed through the CEA2 program (*Chemical Equilibrium with Applications*) [Gordon *et al.* (1994)]. The 1D Riemann problem is implemented in a shock tube of length equal to 14 m. The origin of coordinates x is placed in the middle of the tube. In all cases, except the case D, the initial discontinuity position coincides with the origin of coordinates. In the case D, the initial discontinuity is placed in $x = -1.0$. The results presented in Figs. 1–5 were obtained through a discretization of 100 cells of constant length $\Delta x = 0.14$ m. The CFL number CFL$= \Delta t/\Delta x \max(|u_i| + c_i)$ is

Table 1. Initial conditions of test cases.

Case	State	Density (kg/m^3)	Pressure (N/m^2)	Temp. (K)	Velocity (m/s)
A	(L)	0.0660	9.84×10^4	4390.8	0.0
	(R)	0.0300	1.50×10^4	1741.8	0.0
B	(L)	1.4000	9.88×10^5	2456.5	0.0
	(R)	0.1400	9.93×10^3	247.1	0.0
C	(L)	1.2900	1.00×10^5	270.0	0.0
	(R)	0.0129	1.00×10^4	2648.9	0.0
D	(L)	1.0000	6.50×10^5	2263.6	0.0
	(R)	0.0100	1.00×10^3	348.4	0.0
E	(L)	0.0100	5.73×10^2	199.6	2200.0
	(R)	0.1400	2.23×10^4	554.9	0.0

selected equal to 0.75 and the entropy fix parameter δ_1 in (9) is selected to be a constant equal to 0.10 in all cases. The boundary conditions are treated through the ghost cell technique, and are considered as transmissive in all cases.

4.2. *Numerical experiments*

A comparison between the results obtained through the use of three schemes is carried out. The scheme (a) employs the *minmod* (11) limiter function with all waves. The scheme (b) uses the *minmod* limiter function with the nonlinear degenerated characteristic waves and the *superbee* (12) limiter function with the linearly degenerated wave. The adaptive scheme (c) is the one proposed in [Falcinelli *et al.* (2008)]. In this one, the strengths of the waves $I^{(l)}$ defined in (10) are first evaluated. If the maximum of the strength of the nonlinear degenerated waves is greater than the strength of the linearly degenerate wave, then scheme (a) is employed at this interface, otherwise the flux defined by the scheme (b) is employed.

In addition, the numerical solutions are compared with a pseudo analytic solution of the Riemann problem, obtained according to the methodology proposed in [Saurel *et al.* (1994)]. The results of the L_2-norm of the error in density with respect to this analytic solution are presented in Table 2 for discretizations of 100, 200, 500 and 1000 cells respectively.

4.2.1. *Test case A*

In test case A (Fig. 1), the wave system of the Riemann problem consists in a rarefaction wave that travels to the left, a contact discontinuity and a shock wave that travels to the right. The three schemes capture the shock wave in a space of three cells, while schemes (b) and (c) resolve significantly better the contact discontinuity. In this test case, and all subsequents test cases, the effects introduced by the thermo–chemical equilibrium assumptions are qualitatively given by the great variations that take place in the γ coefficient. Particularly in this case, a great oscillation appears in the γ coefficient at the contact discontinuity. The schemes (b) and (c) do not change the amplitude of the oscillations but they appreciably reduce its spread out. This oscillation is of thermodynamic nature, and represents a minimum of the function γ corresponding to the thermodynamic states numerically obtained behind the wave. Finally, it can be observed that the scheme (b) and the adaptive scheme (c) do not show appreciable differences.

4.2.2. *Test case B*

In this case (Fig. 2) the wave system is similar to the case A, but with stronger shocks, and with a weaker contact discontinuity. Again, the three schemes solve the shock wave in a space of three cells, while the two schemes that use the *superbee* function improve the resolution at the contact discontinuity without introducing appreciable oscillations. In this case, the γ coefficient is monotonically decreasing to

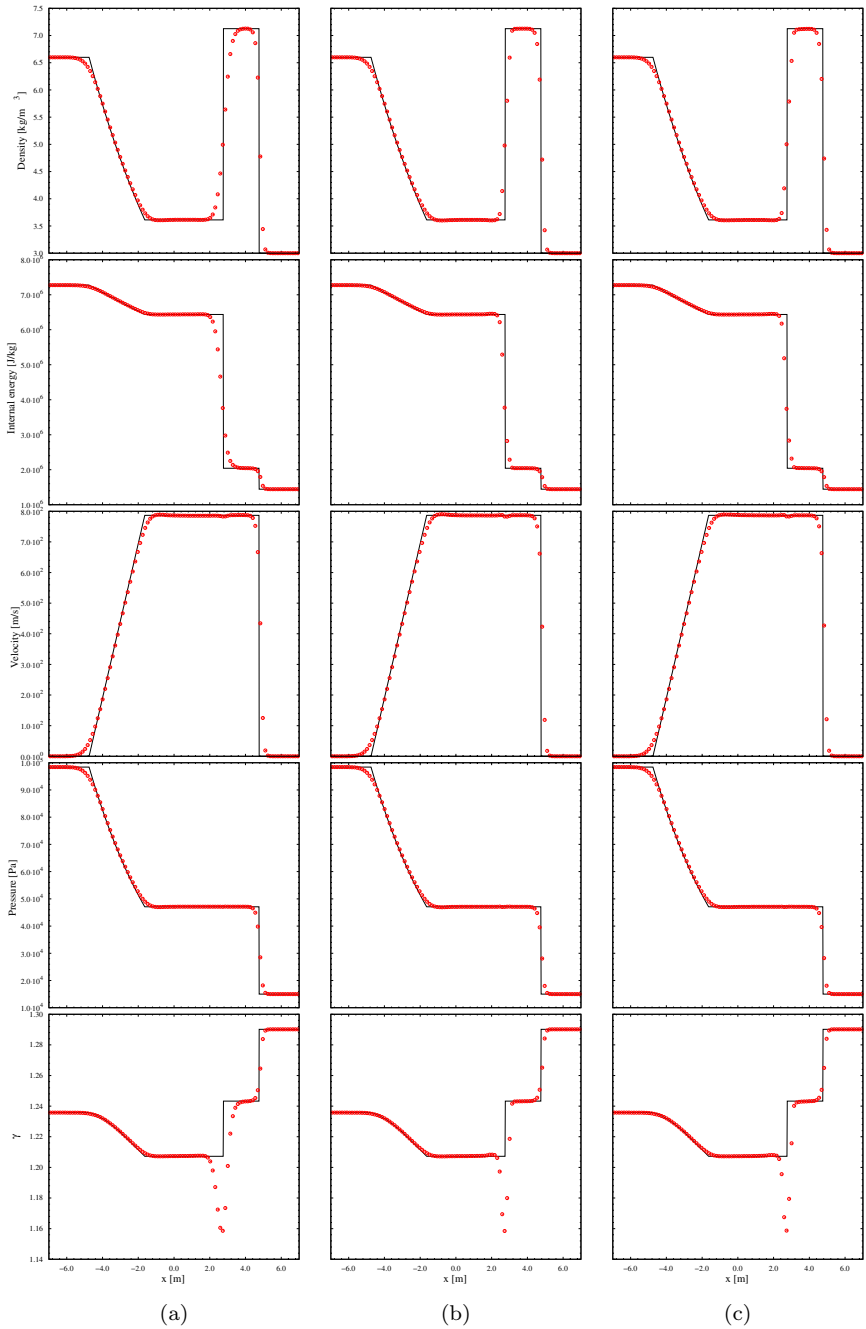

Fig. 1. Comparison of the TVD schemes considering chemical equilibrium gas for the test case A. Output time: 3.5 ms. (a) Minmod in all waves, (b) Nonadaptive scheme and (c) New adaptive scheme.

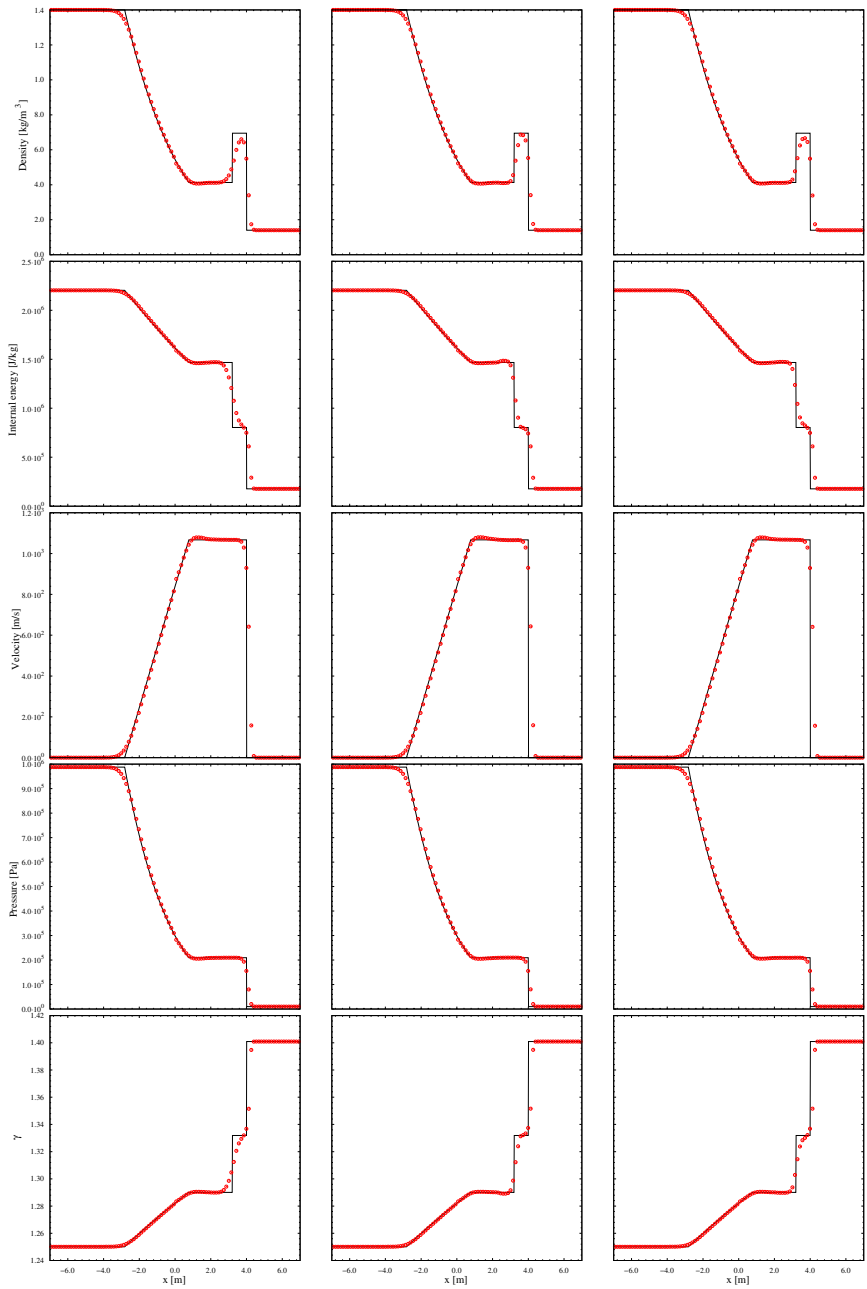

Fig. 2. Comparison of the TVD schemes considering chemical equilibrium gas for the test case B. Output time: 3.5 ms. (a) Minmod in all waves, (b) Nonadaptive scheme and (c) New adaptive scheme.

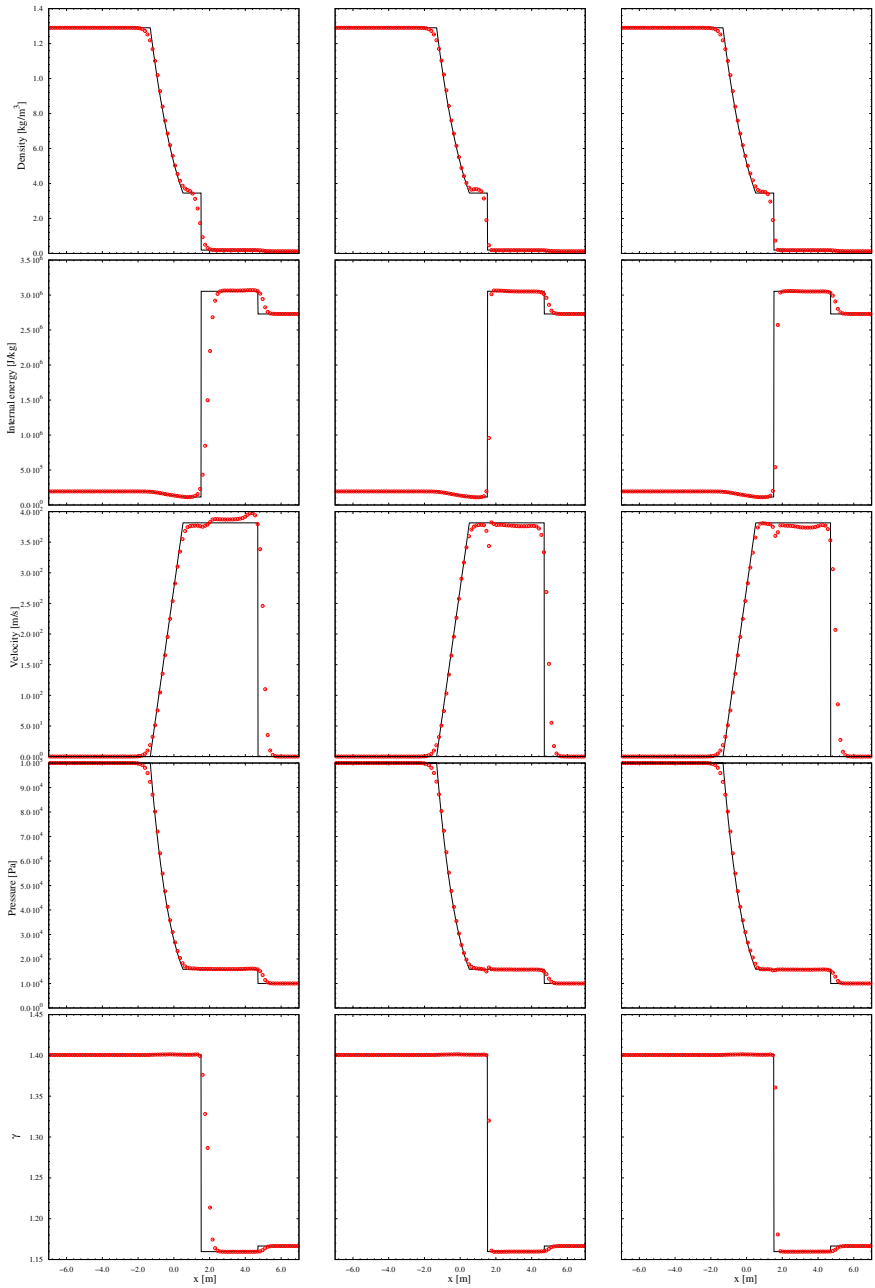

Fig. 3. Comparison of the TVD schemes considering chemical equilibrium gas for the test case C. Output time: 3.0 ms. (a) Minmod in all waves, (b) Nonadaptive scheme and (c) New adaptive scheme.

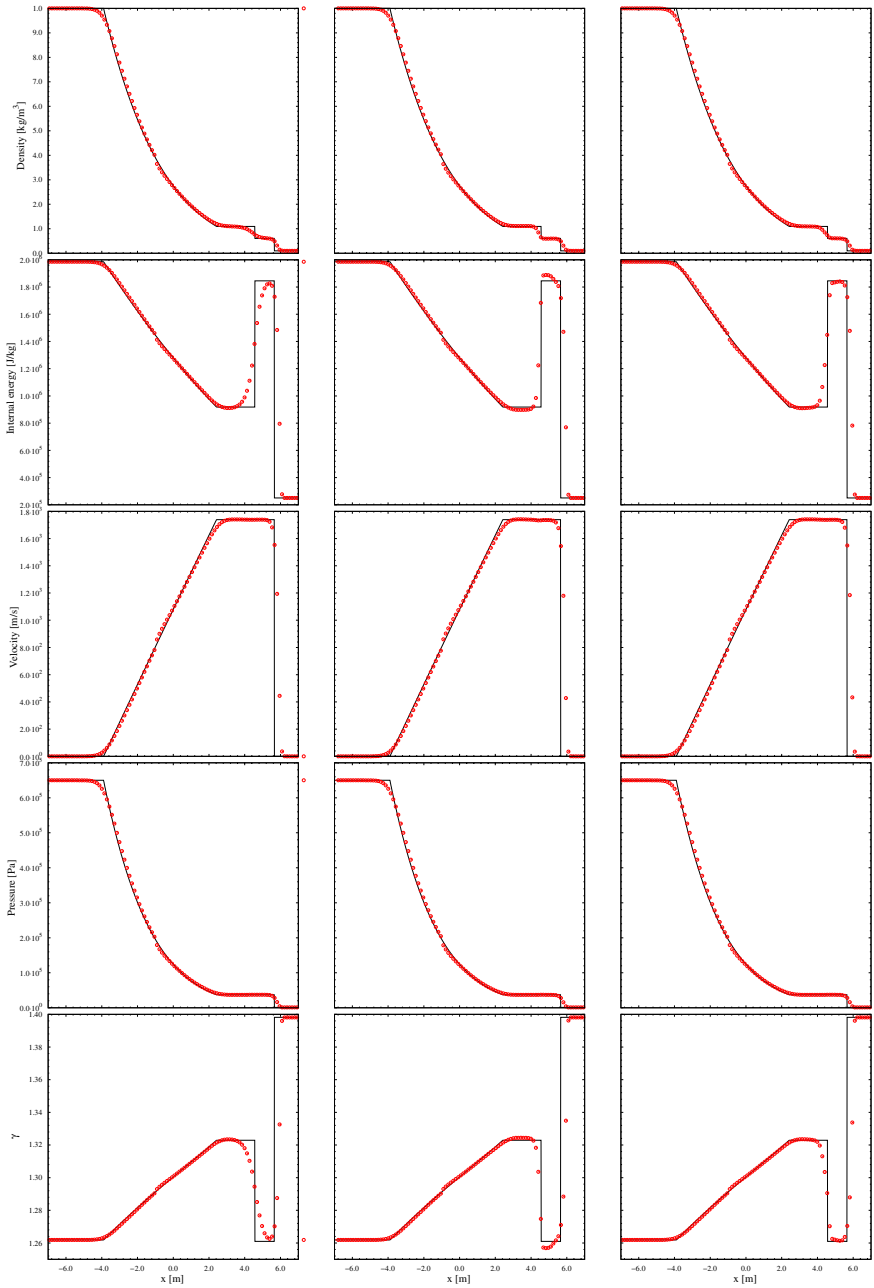

Fig. 4. Comparison of the TVD schemes considering chemical equilibrium gas for the test case D. Output time: 4.0 ms. (a) Minmod in all waves, (b) Nonadaptive scheme and (c) New adaptive scheme.

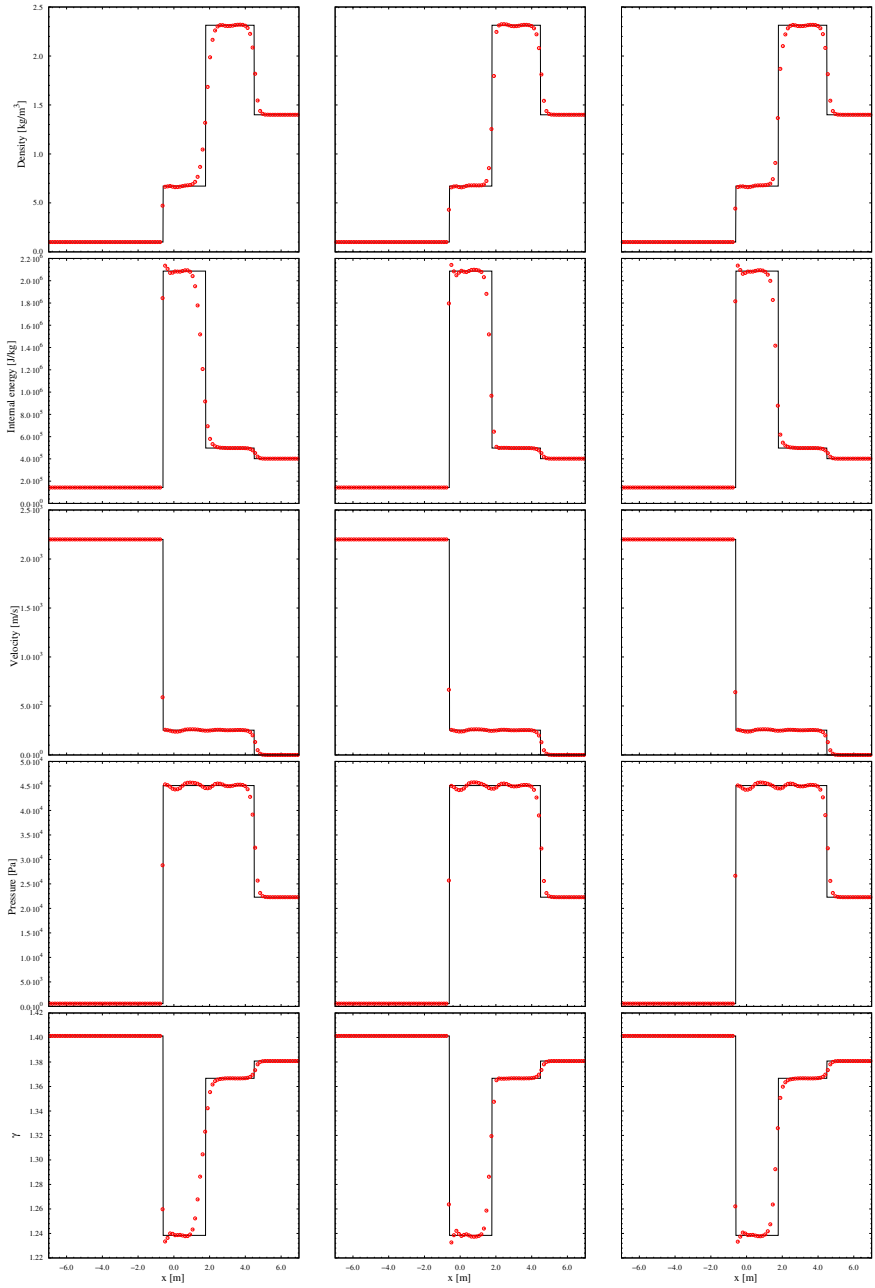

(a) (b) (c)

Fig. 5. Comparison of the TVD schemes considering chemical equilibrium gas for the test case E. Output time: 3.2 ms. (a) Minmod in all waves, (b) Nonadaptive scheme and (c) New adaptive scheme.

Table 2. L_2-norm of the solution errors of density.

Nodes	Scheme A	Scheme B	Scheme C
Test case A			
100	0.5701E-02	0.3954E-02	0.4044E-02
200	0.3182E-02	0.2274E-02	0.2278E-02
500	0.1413E-02	0.8926E-03	0.8791E-03
1000	0.7449E-03	0.3647E-03	0.3688E-03
Test case B			
100	0.6081E-02	0.5709E-02	0.5290E-02
200	0.3996E-02	0.3602E-02	0.3569E-02
500	0.1634E-02	0.1762E-02	0.1528E-02
1000	0.8682E-03	0.7363E-03	0.7205E-03
Test case C			
100	0.1584E-01	0.8773E-02	0.9134E-02
200	0.8905E-02	0.5162E-02	0.5163E-02
500	0.4198E-02	0.3893E-02	0.3280E-02
1000	0.2181E-02	0.7509E-03	0.8842E-03
Test case D			
100	0.1129E-01	0.1495E-01	0.1338E-01
200	0.4627E-02	0.7360E-02	0.6108E-02
500	0.1912E-02	0.6800E-02	0.3873E-02
1000	0.1223E-02	0.7003E-02	0.2938E-02
Test case E			
100	0.11307E-01	0.9474E-02	0.9980E-02
200	0.4996E-02	0.3690E-02	0.3353E-02
500	0.2372E-02	0.1564E-02	0.1357E-02
1000	0.1447E-02	0.9466E-03	0.9930E-03

internal energy, in all the computational domain. This behavior is also encountered in the subsequent cases. As in test case A, no appreciable differences are encountered between the results obtained using schemes (b) and (c).

4.2.3. *Test case C*

The case C (Fig. 3) presents a wave system similar to the previous one characterized by the presence of an intense and slow contact discontinuity, a weak shock and a strong transonic expansion. All schemes over estimate the shock speed. The scheme (a) also over estimate the contact discontinuity velocity, while schemes (b) and (c) considerably improve its resolution. An appreciable overshoot in the velocity behind the right shock wave is present in scheme (a) that is almost absent in schemes (b) and (c). Some oscillations in the pressure and velocity are introduced with the superbee limiter near the contact wave that are somewhat reduced with the adaptive scheme.

4.2.4. *Test case D*

The case D (Fig. 4) presents a large transonic expansion wave, a contact discontinuity and a shock wave both with high jumps in internal energy values, but with small

jumps in density. An over estimation and oscillations in the internal energy at the contact wave are detected applying scheme (b). However, both of them are damped with the adaptive scheme. This is the test case where best noticeable improvements introduced by the adaptive scheme are noticed.

4.2.5. *Test case E*

The case E (Fig. 5) presents a slow left traveling shock and fast right traveling contact and shock waves. The capture of the nearly stationary left shock is practically exact with the three schemes as a consequence of using the Roe's Riemann solver. An oscillatory behavior behind the slowly moving shock waves appears [Roberts (1990)]. No improvements are achieved as a result of introducing the *superbee* limiter in this test case.

4.3. *General discussion*

The numerical experiments carried out have shown that the limiter function *superbee*, applied only to the contact wave, has no influence on the capture of shock waves, but significantly improves the capture of contact discontinuities. However, it is well known that the *superbee* limiter introduce oscillations in regions next to the contact wave, which magnitude and influence zone depends on the wave speed, wave strength and the interaction with other waves. On the other hand, the introduction of the function *superbee* in an adaptive fashion has reduced this oscillations without loosing resolution in two of the five test cases presented here. For the other three cases, there are no appreciably differences between schemes (b) and (c). It can be inferred that in those cases where the superbee limiter introduce oscillations near the contact discontinuity while the minmod limiter does not, the introduction of superbee in an adaptive fashion will likely result in a damping of this oscillations without compromising the resolution of the contact wave. Furthermore, these advantages are obtained at negligible additional computational costs.

5. Conclusion

The TVD finite volume solver for the 1D Euler's equations proposed by [Falcinelli *et al.* (2008)] has been extended to account for the state of the gas in chemical equilibrium. This solver, based on the Yee generalization [Yee *et al.* (1985)] of the original Harten scheme [Harten *et al.* (1983b)] employs selectively the *superbee* limiter function with the linearly degenerate waves and the *minmod* limiter function with the rest. This requires the previous determination of those regions of the domain where the strength of the linearly degenerate waves is greater than the genuinely nonlinear ones. Otherwise, the *minmod* function is applied to all waves. This technique aims to improve the capture of contact discontinuities through more compressive limiter functions, while keeping the robustness that it is achieved through

more diffusive limiter functions. Results corresponding to five 1D Riemann problems specially designed to account for chemical equilibrium effects were presented. To test the usefulness of the proposed adaptive technique, comparisons were made with the original Yee's TVD scheme and with a nonadaptive one that always uses the *superbee* limiter in the linearly degenerate waves. In all test cases, the *superbee* limiter improves significantly the resolution of contact discontinuities and does it without altering the capture of nonlinear waves. However, in those cases where the *superbee* limiter induces in the flow variables nonphysical oscillations in regions next to the contact wave while the *minmod* limiter does not, the proposed adaptive technique reduces this oscillations without altering the resolution of the contact wave. Finally, it can be concluded that the proposed technique works satisfactorily when thermo–chemical equilibrium gas assumptions are considered.

Acknowledgments

The authors are indebted to the UNC, MCyT Córdoba and CONICET for financial support and to Gustavo Scarpín of Aeronautical Universitary Institute for the use of subroutines of his authorship.

References

Anderson, J. D. [1989] *Hypersonic and High Temperature Gas Dynamics* (McGraw-Hill Book Co., New York, 1989).

Falcinelli, O., Elaskar, S. and Tamagno, J. [2008] "Reducing the numerical viscosity in non structured three-dimensional finite volume computations," *J. Spacecr. Rocket* **45**, 506–509.

Gordon, S. and McBride, J. B. [1994] "Computer program for calculation of complex equilibrium compositions and applications. Part I: Analysis," NASA RP 1311.

Harten, A. [1983] "On a class of high resolution total-variation–stable finite-difference schemes," *J. Comput. Phys.* **49**, 357–393.

Harten, A. and Hyman, J. M. [1983] "Self adjusting grid methods for one–dimensional hyperbolic conservation laws," *J. Comput. Phys.* **50**, 235–269.

Hirsch, C. [1992] *Numerical Computation of Internal and External Flows*, Vol. 2 (John Wiley & Sons Ltd, Oxford, 1992).

Montagné, J. L., Yee, H. C. and Vinokur, M. [1989] "Comparative study of high–resolution shock–capturing schemes for a real gas," *AIAA J.* **27**, 1332–1346.

Mottura, L., Vigevano, L. and Zaccanti, M. [1997] "An evaluation of Roe's scheme generalizations for equilibrium real gas flows," *J. Comput. Phys.* **138**, 354–399.

Roberts, T. W. [1990] "The behavior of flux difference splitting schemes near slowly moving shock waves," *J. Comput. Phys.* **90**, 141–160.

Roe, P. L. [1981] "Approximate Riemann solvers, parameter vectors, and difference schemes," *J. Comput. Phys.* **45**, 357–372.

Roe, P. L. [1986] "Characteristic-based schemes for the Euler equations," *Ann. Rev. Fluid Mech.* **18**, 337–365.

Saurel, R., Larini, M. and Loraud, J. C. [1994] "Exact and approximate Riemann solvers for real gases," *J. Comput. Phys.* **112**, 126–137.

Sweby, P. [1984] "High resolution schemes using flux limiters for hyperbolic conservation laws," *SIAM J. Numer. Anal.* **21**, 995–1011.

Vinokur, M. and Montagné, J. L. [1990] "Generalized flux-vector splitting and Roe average for an equilibrium real gas," *J. Comput. Phys.* **89**, 276–300.

Yee, H. C. [1987a] "Upwind and symmeric shock–capturing schemes," NASA TM 89464.

Yee, H. C. [1987b] "Construction of explicit and implicit symmetric TVD schemes and their applications," *J. Comput. Phys.* **68**, 151–179.

Yee, H. C. [1989] "A class of high–resolution explicit and implicit shock-capturing methods," NASA TM 101088.

Yee, H. C., Warming, R. and Harten, A. [1985] "Implicit total variation diminishing (TVD) schemes for steady–state calculations," *J. Comput. Phys.* **57**, 327–360.

Zheng, B. and Lee, C. H. [1998] "The effects of limiters on high resolution computations of hypersonic flows over bodies with complex shapes," *Comm. Nonlinear Sci. Numer. Simul.* **3**(2), 82–87.